

Sequential C–H Arylation and Enantioselective Hydrogenation Enables Ideal Asymmetric Entry to the Indenopiperidine Core of an 11 β -HSD-1 Inhibitor

Xudong Wei,^{*,†} Bo Qu,^{*,†} Xingzhong Zeng,[†] Jolaine Savoie,[†] Keith R. Fandrick,[†] Jean-Nicolas Desrosiers,[†] Sergei Tcyrulnikov,[‡] Maurice A. Marsini,[†] Frederic G. Buono,[†] Zhibin Li,[†] Bing-Shiou Yang,[†] Wenjun Tang,[†] Nizar Haddad,[†] Osvaldo Gutierrez,[‡] Jun Wang,[†] Heewon Lee,[†] Shengli Ma,[†] Scot Campbell,[†] Jon C. Lorenz,[†] Matthias Eckhardt,[§] Frank Himmelsbach,[§] Stefan Peters,[§] Nitinchandra D. Patel,[†] Zhulin Tan,[†] Nathan K. Yee,[†] Jinhua J. Song,[†] Frank Roschangar,[†] Marisa C. Kozlowski,[‡] and Chris H. Senanayake[†]

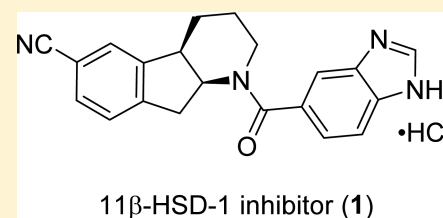
[†]Chemical Development, Boehringer Ingelheim Pharmaceuticals, Inc., 900 Ridgebury Road, Ridgefield, Connecticut 06877, United States

[‡]Department of Chemistry, University of Pennsylvania, Philadelphia, Pennsylvania 19104, United States

[§]Medicinal Chemistry, Boehringer Ingelheim Pharma GmbH & Co. KG, Birkendorfer Strasse 65, 88397 Biberach/Riss, Germany

S Supporting Information

ABSTRACT: A concise asymmetric synthesis of an 11 β -HSD-1 inhibitor has been achieved using inexpensive starting materials with excellent step-economy at low catalyst loadings. The catalytic enantioselective total synthesis of **1** was accomplished in 7 steps and 38% overall yield aided by the development of an innovative, sequential strategy involving Pd-catalyzed pyridinium C–H arylation and Ir-catalyzed asymmetric hydrogenation of the resulting fused tricyclic indenopyridinium salt highlighted by the use of a unique P,N-ligand (MeO-BoQPhos) with 1000 ppm of [Ir(COD)Cl]₂.



INTRODUCTION

Type 2 diabetes is a metabolic disorder characterized by hyperglycemia, insulin resistance, and relative insulin deficiency.¹ The global prevalence of diabetes was estimated to be 9% in 2014 among adults and is projected to increase annually.² In the search for an effective therapeutic agent to curb this global epidemic, inhibition of the sodium-dependent glucose cotransporter enzyme, 11 β -hydroxysteroid dehydrogenase type 1 (11 β -HSD-1), has been investigated as a clinically relevant tactic for reduction of cortisol production in various tissues believed to be responsible for obesity and insulin resistance in children and adults. To this end, compound **1** emerged from our discovery program as a potent, metabolically stable 11 β -HSD-1 inhibitor³ and has quickly advanced in clinical trials.

Compound **1** contains an intriguing tricyclic chiral indenopiperidine core that has also been observed in several other biologically active molecules and alkaloid natural products.⁴ Despite its relatively small molecular size and the deceptively simple structure, the architecturally unusual tricyclic indenopiperidine nucleus containing two embedded contiguous stereogenic centers presented a formidable synthetic challenge. Indeed, the first-generation route toward **1** required 12 linear steps to construct tricyclic core **2** starting from 2,3-dichloropyridine.³ The lengthy, racemic synthesis relies on a Pd-catalyzed cyanation with Zn(CN)₂ and a late-stage resolution to supply drug candidate for early toxicological

studies. The overall yield for the synthesis of **1** was less than 3% over a total of 15 steps with poor atom efficiency. In order to provide large quantities of compound for accelerated clinical studies (>3 tons for Phase III), a more efficient and economical synthesis was urgently required.

Herein, we describe our design and development of a concise asymmetric route to 11 β -HSD-1 inhibitor **1** based on the successful, sequential implementation of an intramolecular C–H pyridinium arylation and enantioselective hydrogenation of the resulting fused indenopyridinium salt enabled by Boehringer Ingelheim's P,N-ligand BoQPhos.^{5,6}

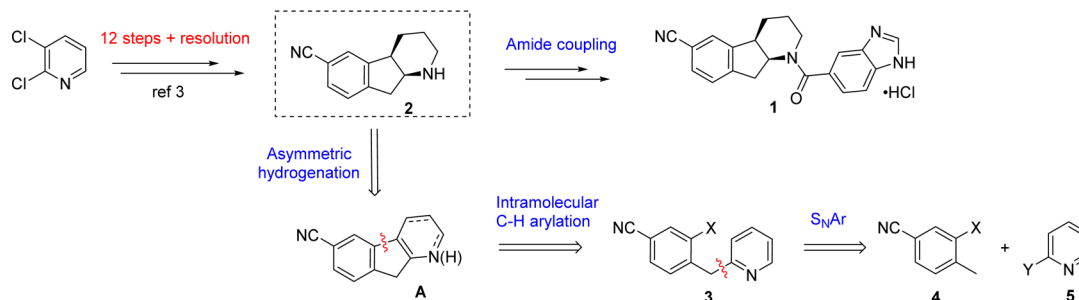
RESULTS AND DISCUSSION

Retrosynthetic Analysis. Chiral piperidines are common structural motifs exhibited in natural products and highly pursued in drug discovery; in this vein, numerous synthetic methodologies have been reported.⁷ In designing an ideal synthesis⁸ for compound **1**, a synthetic strategy was crafted in order to provide the shortest possible synthetic route to the target molecule by taking full advantage of catalytic technologies to drive down cost and effectively increase throughput of the synthesis.

Received: September 18, 2016

Published: October 30, 2016

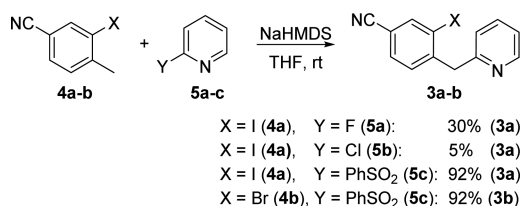
Scheme 1. Fifteen-Step Discovery Approach and New Streamlined Retrosynthesis toward 1



Tactically, synthetic approaches to piperidines utilizing pyridines as starting materials became attractive due to their high abundance and low cost. We envisioned that the two stereogenic centers at the piperidine ring juncture could be introduced via a catalytic asymmetric hydrogenation of a tetra-substituted double bond as part of a piperidine or pyridine ring (Scheme 1, synthon A). Fully aware of the challenges associated with the asymmetric hydrogenation of tetra-substituted olefins,⁹ we aspired to engineer a new catalytic system for this important transformation by leveraging our recently developed dihydrobenzooxaphosphole (BOP)-based ligand series (*vide infra*).^{10,11} To access requisite hydrogenation precursor A, a conceptually concise sequence was devised involving an S_NAr coupling of fragments 4 and 5 followed by an intramolecular C–H arylation. At the outset, the proposed cyclization to the C-3 position of pyridine was expected to be challenging, with few related examples found in the literature.^{12,13} However, if successful, then an expedient route to the key intermediate 2 could be developed from the simple and inexpensive starting materials.

Synthesis of Pyridine Precursors for Cyclization. 2-Benzyl-substituted pyridines are highly valuable compounds in organic synthesis. Existing synthetic approaches employ elaborate starting materials and require either high reaction temperatures or the use of Pd catalysts at high loadings,¹⁴ both of which negatively impact development of a cost-effective process. The S_NAr coupling reaction between 3-iodo-4-methylbenzonitrile 4a and 2-fluoropyridine 5a was first examined in order to prepare the requisite benzylpyridine precursor 3 for cyclization; however, 30% yield was observed with significant amount of self-condensation side products. Switching to 2-chloropyridine 5b provided again trace product formation (Scheme 2).

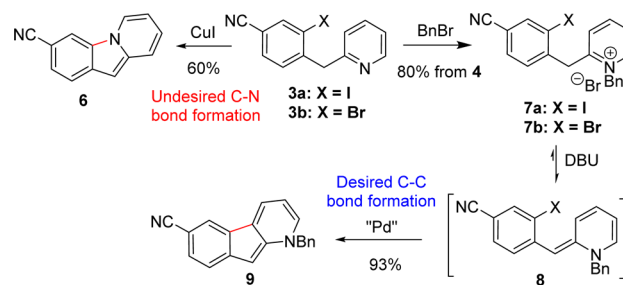
Prior experience from our laboratories¹⁵ has shown that the reaction between a carbanion and a sulfonylpyridine is an efficient method for construction of pyridine derivatives; this guided our investigations toward the coupling of 4a with 5c. To our delight, the reaction occurred smoothly in the presence of NaHMDS at room temperature in high yield after 2 h, allowing

Scheme 2. S_NAr Reaction of Nitrile 4 with 2-Substituted Pyridine Electrophiles

facile access to the key intermediates 3a–b in a straightforward and economical fashion.

Pd-Catalyzed C–H Arylative Cyclization. With compound 3 in hand, the key intramolecular cyclization was investigated next. Direct intramolecular C–H arylation of heteroarenes has become an increasingly popular approach for the construction of fused aromatic structures due to the inherent cost advantages.^{12,13} However, C–H arylation of pyridines has remained an outstanding challenge, especially in an intramolecular fashion. To the best of our knowledge, literature precedent for this type of cyclization to forge the indenopyridine scaffold is nonexistent. Indeed, initial attempts to achieve this cyclization employing 3a as substrate using Pd or Cu catalysts failed to deliver the desired indenopyridine product; undesired C–N bond formation generated 6 as the sole product (Scheme 3).

Scheme 3. Pd-Catalyzed C–H Arylative Cyclization



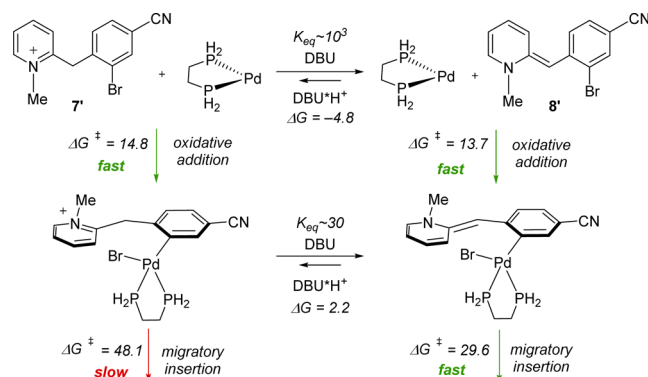
To circumvent this undesired pathway, pyridine *N*-alkylation and acylation were pursued as a means to block C–N bond formation and potentially facilitate formation of benzylpyridinylidene benzonitrile 8 via deprotonation, which, in turn, allows access to a cyclization via a Heck type manifold. *N*-Acylation of pyridine 3 with phenyl chloroformate, however, was unsuccessful due to nonregioselective C-acylation at the benzylic position. Fortunately, crystalline pyridinium salts 7a and 7b could be directly isolated after benzylation with BnBr at 75 °C in high yields, providing a convenient means for purification following the S_NAr coupling. An overall yield of >80% was readily achieved on metric ton scale by performing the S_NAr coupling and benzylation in a single batch to obtain pyridinium salts 7a and 7b as white crystalline solids with >99% purity.

The pyridinium salts 7a,b were then subjected to cyclization with Pd catalysts. In the presence of Pd(OAc)₂, weaker organic bases (Et₃N or *i*-Pr₂NEt) afforded low conversion even under forcing conditions. However, stronger base DBU provided desired tricyclic structure 9 with complete consumption of 7a,b. The highly conjugated neutral species 8¹⁶ was observed as an

intensely red-colored compound upon treatment of **7a,b** with DBU. A detailed screening of Pd catalysts and reaction conditions for the economically preferred aryl bromide **7b** identified Pd(dppf)Cl₂ as the best catalyst system. With 1.25 mol % Pd(dppf)Cl₂ and 3 equiv of DBU in DMF at 110 °C for 2–5 h, highly conjugated indenopyridine **9** was obtained as a deep-red crystalline solid in 93% yield and >99% purity after direct crystallization from the crude reaction mixture. This novel and direct C–H arylation enabled the construction of the requisite tricyclic indenopyridine structure in a concise and highly efficient manner, and was successfully implemented for production of compound **9** in >1 t quantities. Moreover, this work further serves as the basis for development of a nickel catalyzed intramolecular arylation as a general method for the synthesis of 1-azafluorenes.^{17,18}

Mechanistically, the intramolecular cyclization can occur through either neutral intermediate **8** or cationic pyridinium salt **7b** (Scheme 4). To fully understand the mechanism while

Scheme 4. Equilibria and Key Reaction Barriers for Pd-Catalyzed Cyclization^a



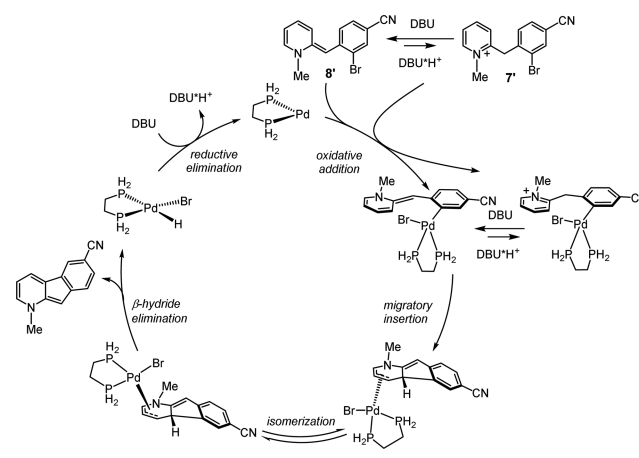
^aComputed using the basis set M06/6-311+G(d,p)-LANL2DZ(Pd)-SMD-nitromethane//B3LYP/6-31G(d)/LANL2DZ(Pd)-gas; values in kcal/mol.

optimizing for process robustness, DFT calculations were performed with Gaussian 09¹⁹ at the B3LYP/6-31G(d)-LANL2DZ(for Pd) level in the gas phase.²⁰ With DBU, free base form **8**/DBU·H⁺ was computed to be 4.8 kcal/mol lower in energy than **7b**/DBU, consistent with **8** being the major species in solution (see below, benzyl replaced with methyl for all intermediates). Notably, computations (see the Supporting Information) revealed that this situation is dependent on both the nitrile substitution acidifying the pyridinium and the use of a stronger amine base DBU in accord with experimental findings.

Both **7b** and **8** were found to undergo facile oxidative addition to the corresponding aryl palladium species, in contrast to the related nickel system where oxidative addition to the pyridinium species is markedly lower in energy.¹⁷ Although significant amounts of both aryl palladium species are expected based on the computed equilibrium for the acid–base interchange, the subsequent migratory insertion onto a double bond of the charged species is untenable (48.1 kcal/mol) due to the aromatic stabilization of the pyridinium. However, the energetic barrier (29.6 kcal/mol) for migratory insertion of the neutral species is readily accessible under the reaction conditions of this process.

The set of equilibria prior to migratory insertion is consistent with the reaction kinetics, and the reaction is expected to be first-order in Pd catalyst and zero-order in substrate (see the Supporting Information). Moreover, since the deprotonation equilibria control the concentration of the preinsertion intermediates, a fractional order in base is expected. The catalytic cycle proposed based on the reaction kinetics and computational results is shown in Scheme 5. Base-mediated

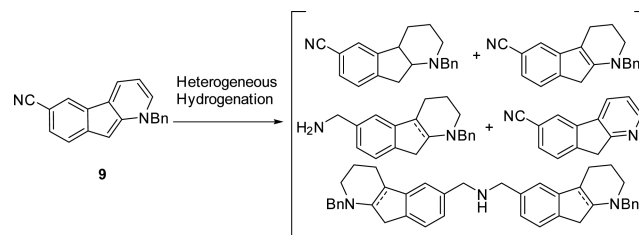
Scheme 5. Proposed Catalytic Cycle for Pd-Catalyzed Cyclization



deprotonation sets up an equilibrium favoring neutral species **8'**, which undergoes oxidative addition of the catalyst. Alternately, oxidative addition to pyridinium form **7'** followed by base mediated-deprotonation generates the same neutral precursor required for the migratory insertion to occur. Isomerization to a syn configuration then facilitates β -hydride elimination to yield the cyclization product and generate a Pd^{II} species that reforms the Pd⁰ catalyst closing the catalytic cycle. Although a lower energy pathway is calculated for free base **8**, we speculate that the higher yields obtained from pyridinium salt **7b** are due to its greater stability, mitigating byproduct formation.¹⁶

Nonenantioselective Hydrogenation and Chiral Resolution. With a concise approach to the highly conjugated tricyclic indenopyridine **9** in hand, we next focused our attention on the desired ring reduction (Scheme 6).

Scheme 6. Challenging Hydrogenation of Indenopyridine **9**

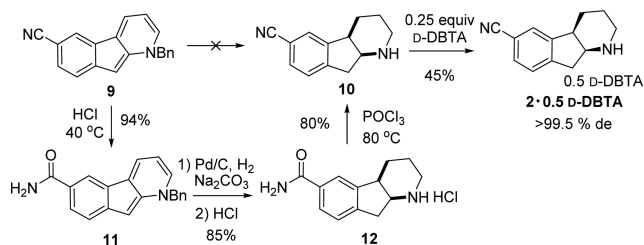


Unfortunately, extensive evaluation of the reduction of **9** in the presence of a range of heterogeneous catalysts (Pd/C, Pt/C, Raney Ni, Rh/C, and Ru/C) clearly indicated that the cyano moiety is incompatible under these conditions. A complex reaction mixture was always obtained as a combination of partial ring reduction, debenzylation, and nitrile reduction.

In view of these significant challenges and urgent material requirements during early stages of development, we pursued a

temporary solution in which the nitrile group was selectively hydrolyzed to the corresponding amide as a protection step, followed by ring reduction/debenzylation and subsequent restoration of the nitrile group by amide dehydration (Scheme 7). Even though no nitrile hydrolysis occurs under forcing basic

Scheme 7. Resolution Route via Nitrile “Protection”



conditions (NaOH or KOH), strongly acidic conditions were found to facilitate the desired hydration. The corresponding amide was cleanly generated in 24 h by using HCl in dioxane. Highly conjugated amide **11** was isolated as a deep red crystalline solid in 94% yield.

Amide **11** was then subjected to hydrogenation conditions for a concomitant pyridine ring reduction and debenzylation. Screening of different types of heterogeneous catalysts identified the optimal conditions with 3 mol % Pd/C in methanol at 80 °C and 200 psi H₂. It was found that addition of Na₂CO₃ induced a mildly basic reaction medium that favored first reduction of the ring and then hydrogenolysis. In this manner, piperidine **12**²¹ was obtained as its hydrochloride salt in ~85% isolated yield. Dehydration with POCl₃ subsequently afforded racemic nitrile **10** as a white crystalline solid in 80% yield. Resolution of piperidine **10** was successfully achieved using 0.25 equiv of *D*-dibenzoyl-tartaric acid (*D*-DBTA). Enantiomerically pure amine salt **2·0.5 D-DBTA** (>99.5% de) was obtained in an excellent isolated yield of 45% (theoretical yield 50%).

Enantioselective Reduction via Known Ligands. In searching for a direct method to convert compound **9** to the reduced product, we postulated that homogeneous hydrogenation could potentially provide better control over chemoselectivity and lead to an enantioselective reduction if the proper chiral ligand was employed. Pioneering work over the past few years on enantioselective reduction of substituted pyridines and heteroarenes was highly encouraging.^{22,23} Nevertheless, most of the strategies are not applicable to the enantioselective hydrogenation of this indeno[1,2-*b*]pyridine system, highlighting the challenges associated with 2,3-disubstituted and fused pyridines. Additionally, industrial applications have not been reported. Indeno[1,2-*b*]pyridine **9** was initially tested in iridium catalyzed asymmetric hydrogenation; reactivity was expected due to the partial aromaticity of the dihydropyridine fragment. Yet it was quickly recognized that compound **9** is not a suitable substrate due to the low reactivity of the highly conjugated system and formation of the dimeric impurities derived from the nonchemoselective reduction of the nitrile moiety.

N-Benzylation of pyridines has recently been shown to activate the substrates for heterocycle reduction and suppress catalyst deactivation via coordination of the nitrogen atom.^{23c,d} In addition, the activated pyridinium salts should, in principle, undergo chemoselective ring reduction even in the presence of a nitrile group. Therefore, we investigated the reduction of pyridinium salt **13**. Different transition metals have been

applied in asymmetric reduction of heteroarenes including ruthenium, rhodium, and iridium catalysts. We first tested the cationic ruthenium diamine catalysts, which have been reported to reduce substituted quinolines with high enantioselectivity.²⁴ Even though highly reactive, large amounts of nitrile reduction were observed and the highest enantioselectivity was at 27% ee (Figure 1).

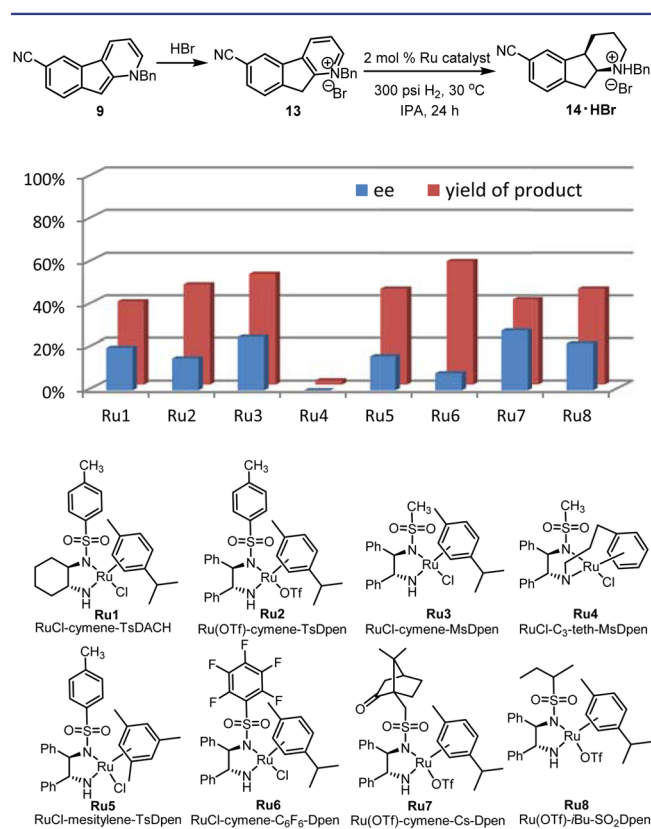


Figure 1. Ruthenium catalysts examined for asymmetric hydrogenation of **13**.

Rhodium bisphosphine catalysts are highly effective for tetrasubstituted alkene reduction²⁵ and have been applied to the reduction of tetrahydropyridine enamine derivative to produce chiral piperidines.²⁶ We thus pursued the asymmetric reduction of pyridinium salt **13** with rhodium catalysts in the presence of different families of chiral phosphine ligands including bisphosphines with axial chirality, Solvias' ferrocene-based ligands, Feringa's monophosphoramidite ligands, and other reported chiral ligands. Disappointingly, both low conversion and low enantioselectivities were observed for all the ligands evaluated (Figure 2). Reactions stalled at different stages of reduction (dihydropiperidine, tetrahydropiperidine, etc.).

Iridium catalysts are known to reduce alkenes without the assistance of any coordinating group on the substrate.²⁷ To facilitate the asymmetric reduction of pyridines, Charette and Legault first demonstrated an activation process for pyridine derivatives by formation of *N*-acyliminopyridinium ylides; effective reduction was achieved applying Pfaltz's PHOX type P₂N₂-ligands.^{23b} Recently Zhou's^{23c} and Zhang's^{23d} groups demonstrated efficient asymmetric pyridine reduction by forming activated *N*-benzylpyridinium salts. A number of monosubstituted 2-aryl derived pyridines were reduced successfully using biaryl ligands with axial chirality including

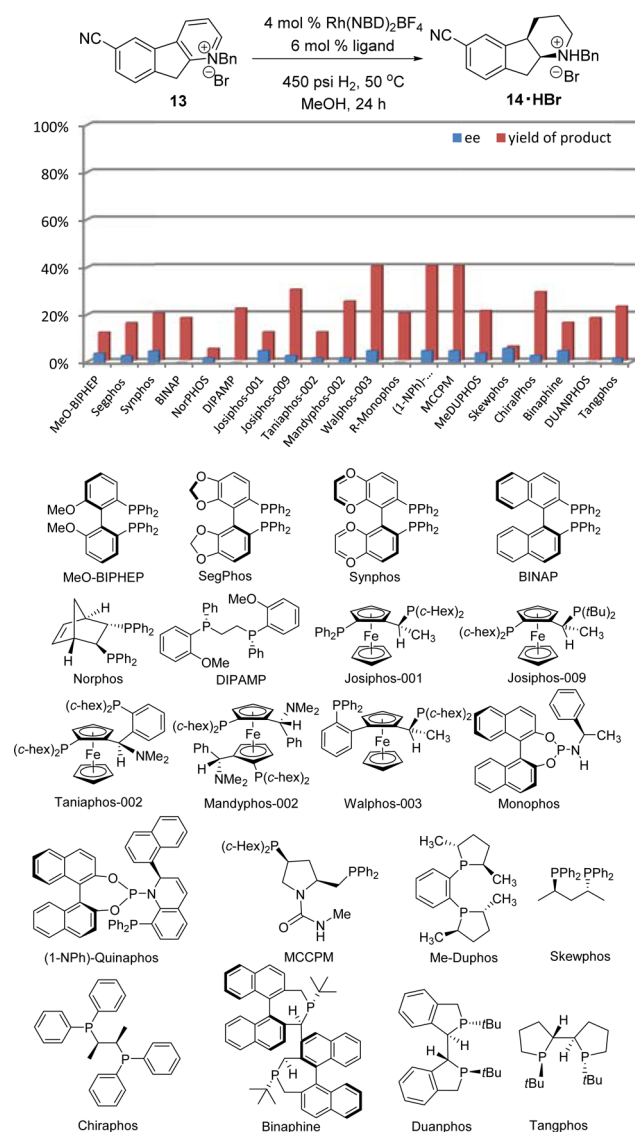


Figure 2. Rhodium catalysts investigated for asymmetric hydrogenation of **13**.

Synphos and MP^2 -Segphos. With *N*-benzylpyridinium salt **13** in hand, we first tested the biaryl ligands. Indeed, promising results were obtained compared to the Ru and Rh catalysts. About 40% ee was observed with Segphos, C3-Tunephos, MeO-biphep, and Synphos ligands. However, comprehensive screening of related ligands did not further improve the enantioselectivity (Figure 3). The best ligand MP^2 -Segphos reported for 2-arylpyridine reduction^{23d} provided only 20% ee. The Solvias' ligands are equally ineffective. In addition to the low enantioselectivity, a major issue was the inability of the catalyst system to fully reduce substrate **13**. When the catalyst loading was decreased to an economically feasible level of 0.1 mol % $[\text{Ir}(\text{COD})\text{Cl}]_2$, less than 15% product formation was observed (last four ligands in bracket). Existing P,N-ligands including PHOX ligands,^{23b} Ph-LalithPhos,²⁸ and BIPI 210²⁹ produced unsatisfactory reactivity and enantioselectivity even with 1 mol % of $[\text{Ir}(\text{COD})\text{Cl}]_2$.

Enantioselective Hydrogenation with BoQPhos Ligands. To overcome the tremendous challenges associated with the desired pyridinium hydrogenation, our efforts shifted toward the development of a new chiral ligand system.

Recently, our group has reported a highly modular dihydrobenzooxaphosphole (BOP) core for ligand design.¹⁰ Many effective ligands have been derived from this motif and have been found to mediate a variety of different catalytic transformations.¹¹ In particular, the rigid bidentate BoQPhos P,N-ligands, which were constructed from the BOP core by anchoring a less basic nitrogen-containing pyridine fragment onto the carbon atom of the O,P ring system (see Figure 4), have been successfully demonstrated for asymmetric hydrogenation of nonfunctionalized tri- and tetrasubstituted olefins.⁶ Since the presumed final intermediate in the reduction of tricyclic substrate **13** contains a tetrasubstituted double bond (see compound **15** in Figure 3), we anticipated that the BoQPhos series would be applicable to the asymmetric reduction of 2,3-disubstituted pyridinium salts (Figure 4).

In our first approach, pyridinium salt **13** was subjected to hydrogenation conditions in the presence of $[\text{Ir}(\text{COD})\text{Cl}]_2$ and **L1**, which was the best ligand previously found for olefin hydrogenation.⁶ However, limited product formation (10%) and low enantioselectivity (57:43 er) were observed. We postulated that the low reactivity was caused by the steric hindrance from the dimethoxyphenyl moiety on the western hemisphere of the ligand. Indeed, removal of this group (**L2**) increased the desired product to 40% with the same enantioselectivity. To identify the key interactions of the ligand, structural modifications were pursued on both the western aryl and eastern pyridine rings. The substitution on the pyridine ring affects the enantioselectivity significantly. An *ortho*-MeO substitution on pyridine (**L3**) increased the er to 84:16 with 90% yield. The highest enantiomeric ratio of 85:15 was obtained with MeO-BoQPhos (**L5**) containing methoxy substituents on both the aryl and pyridine rings and produced 97% yield of the reduced product. Changing one of the methoxy groups to isopropoxy (**L6** or **L7**) or adding an additional methoxy group on the pyridine ring (**L10**) resulted in slightly decrease in enantioselectivity. As expected, use of nonrigid open-chain ligand **L12** also decreased the enantioselectivity. Gratifyingly, the P,N-ligand is completely chemoselective; the dimeric impurity derived from nitrile reduction was not observed. Furthermore, MeO-BoQPhos is highly reactive in this challenging catalytic asymmetric hydrogenation process, allowing catalyst load to be decreased as low as 0.1 mol % $[\text{Ir}(\text{COD})\text{Cl}]_2$ while still providing 93% isolated yield and 85:15 er, clearly demonstrating the superb activity and robustness of the BOP-pyridine P,N-ligands for the effective asymmetric pyridine reduction. In contrast to the bisphosphine ligands,^{23c,d} the use of iodine as an additive improves both the enantioselectivity and the reactivity of the hydrogenation reaction using the P,N-ligands.

We have also evaluated the pyridinium salts with different counterions including Cl^- , I^- , HSO_4^- , BF_4^- , and PF_6^- . All these salts demonstrated similar enantioselectivity of 85:15 er at high catalyst load of more than 3 mol % iridium.³⁰ For a cost-effective process, low catalyst load at ≤ 1 mol % iridium was further investigated. The chloride salt is highly hygroscopic and was isolated as a monohydrate (containing about 5% water); the unproductive pathways of enamine hydrolysis and condensation become more competitive at low catalyst load. BF_4^- and PF_6^- salts were found to be much more soluble. However, reaction monitoring revealed that lower enantioselectivity was obtained at low catalyst loads, and the enantioselectivity continued to decrease over the course of the reaction (Figure 5). The bromide salt of **13** was eventually

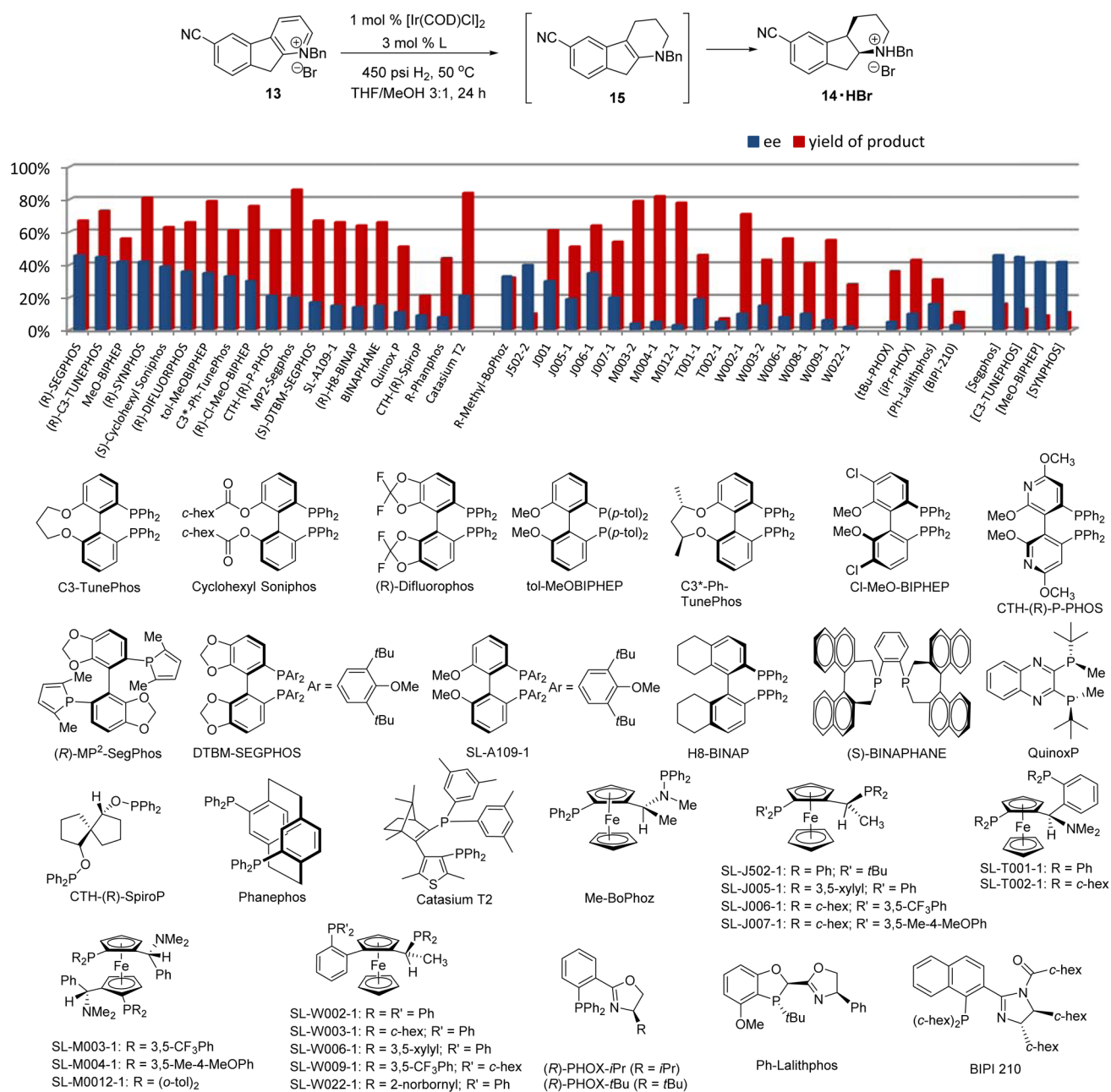


Figure 3. Evaluation of iridium catalysts with known ligands in the asymmetric hydrogenation of **13**. Reaction conditions: 30 mg of **13**, 1.0 mol % $[\text{Ir}(\text{COD})\text{Cl}]_2$, and 3 mol % ligand at 450 psi H_2 and 50 °C in 0.9 mL of THF/MeOH (3:1) for 24 h; I_2 (5 mol %) was added to the mixture of the four P,N-ligands listed in parentheses. The last four ligands in bracket were run at low catalyst load: 0.3 g of **13**, 0.1 mol % $[\text{Ir}(\text{COD})\text{Cl}]_2$, and 0.3 mol % ligand in 5 mL of solvent under the same conditions. Product yield was calculated from quantitative HPLC solution assay of the product **14** upon Et_2NH treatment; ee was obtained on HPLC with a chiral stationary phase.

selected for the process. The optimized conditions with 0.1 mol % $[\text{Ir}(\text{COD})\text{Cl}]_2$ and 0.3 mol % **L5** were successfully applied to deliver the desired product **14**·HBr on multikilogram scale.

The catalytic cycle of this asymmetric hydrogenation process was proposed as an outer-sphere reaction pathway (Figure 6) based on the previously described mechanism of quinoline reduction³¹ and computational studies on the enantio-determining step of key enamine intermediate **15** (Figure 7). The anionic iodo-Ir(III) hydride complex **C** first delivers one hydride to cationic pyridinium salt **13** to afford 1,4-hydride addition product **16** and a catalytic neutral species **D** which then coordinates one hydrogen molecule to generate **B**. Continuous proton transfer from **B** to **16** and hydride transfer

from **C** to **17** produces key enamine intermediate **15**, which undergoes enantio-determining proton transfer and syn hydride delivery to produce *cis*-**14**. The catalyst is regenerated by coordinating hydrogen and proton transfer to yield the protonated amine salt **14**·HBr.

Calculations were conducted with the Gaussian 09¹⁹ program at the DFT level of theory employing B3LYP³² and the LANL2DZ basis set with ECP for Ir²⁰ and D95v for the remaining atoms.³³ An outer-sphere dissociated mechanism³⁴ similar to the DFT-computed Ir-catalyzed hydrogenation mechanism of imines³⁵ and quinolines³¹ was used as the basis for the computational studies of the asymmetric Ir-(S,S-L5)-catalyzed hydrogenation of enamine intermediate **15**. Iodo-

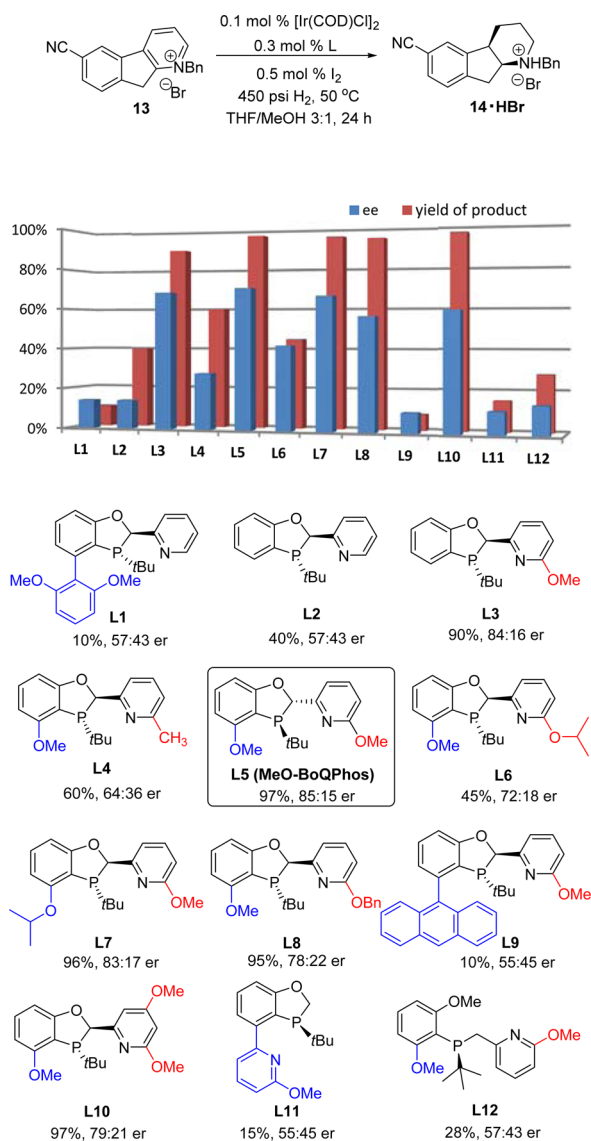


Figure 4. Evaluation of BI's pyridine-containing P,N-ligands for asymmetric hydrogenation of **13**. Reaction conditions: 300 mg of **13**, $0.1 \text{ mol } \% [\text{Ir}(\text{COD})\text{Cl}]_2$, $0.3 \text{ mol } \% \text{ ligand}$, and $0.5 \text{ mol } \% \text{ I}_2$, at 450 psi H_2 and $50 \text{ }^\circ\text{C}$ in 5 mL of THF/MeOH (3:1) for 24 h. Product yield was calculated from quantitative HPLC solution assay of the product **14** upon Et_2NH treatment; ee is measured on HPLC with a chiral stationary phase.

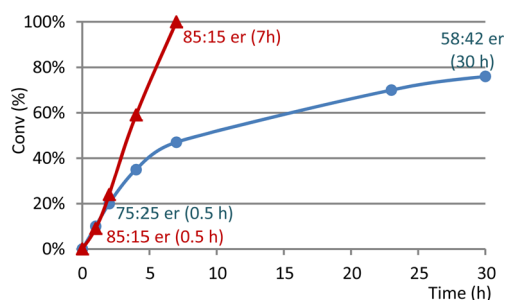


Figure 5. Comparison of asymmetric hydrogenation reaction profiles with low catalyst load. Red: Br^- salt with $0.2 \text{ mol } \% [\text{Ir}(\text{COD})\text{Cl}]_2/0.5 \text{ mol } \% \text{ L5}/1 \text{ mol } \% \text{ I}_2$ at $50 \text{ }^\circ\text{C}$ and 450 psi H_2 ; blue: PF_6^- salt with $0.5 \text{ mol } \% [\text{Ir}(\text{COD})\text{Cl}]_2/1.2 \text{ mol } \% \text{ L5}/2.5 \text{ mol } \% \text{ I}_2$ at $50 \text{ }^\circ\text{C}$ and 450 psi H_2 .

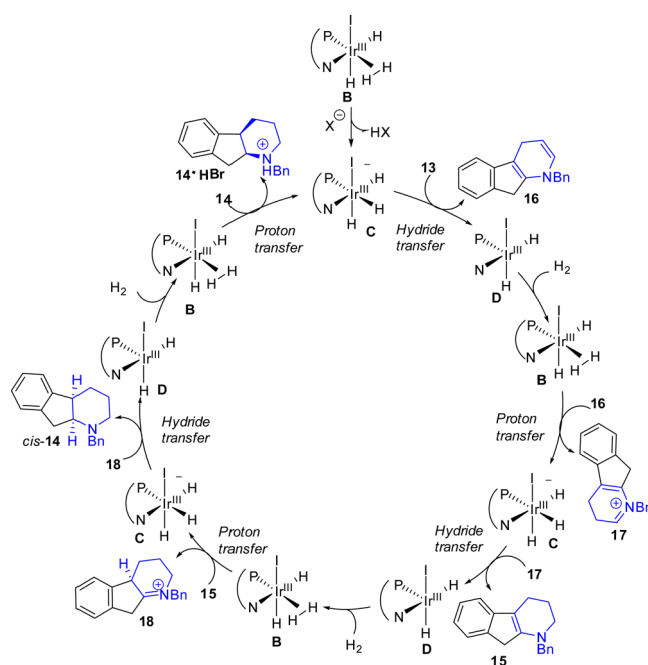


Figure 6. Proposed catalytic cycle of outer-sphere dissociative pathway for asymmetric hydrogenation of **13** (CN group omitted).

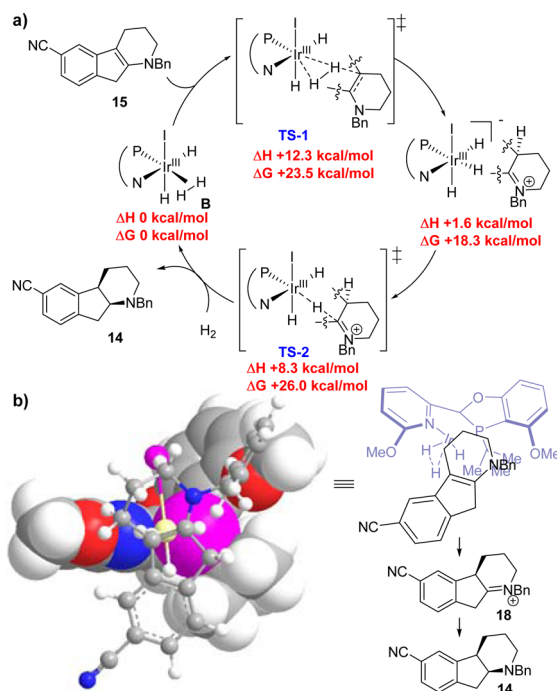


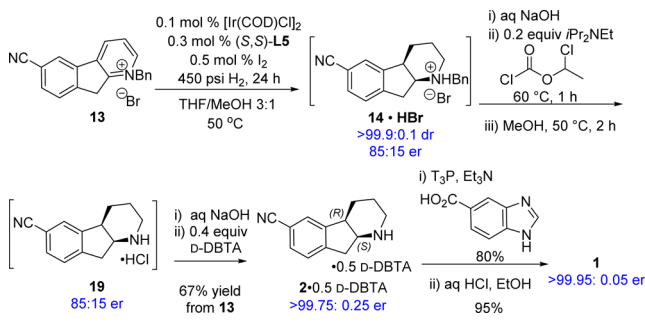
Figure 7. (a) Proposed asymmetric outer-sphere dissociative catalytic cycle of the Ir-Hydrogenation enamine intermediate **15**. DFT calculations: B3LYP/LANL2DZ, CPCM solvation model with THF. Thermal corrections at: 323.15 K at 1 atm. (b) 3D-Model of TS-1 and stereochemical model via syn-Ir-hydride reduction of iminium intermediate **18**.

Ir(III) complex **B** was found to be a viable catalyst for the sequential protonation and hydride delivery pathway for enamine reduction. Although the rate limiting step is hydride delivery (TS-2), the initial hydrogen transfer (protonation) dictates the stereochemical outcome of the transformation (TS-1) as the diastereoselective iridium-hydride delivery would

preferentially occur from the less sterically demanding convex face (syn) directed by the stereocenter of iminium intermediate **18**. This result is consistent with the experimental observation that the addition of the two hydrogens across the double bond in enamine **15** occurs in an exclusively cis fashion, with no trans isomer detected in the reaction mixture.²¹

Completion of the Synthesis. With enantioenriched indenopyridine **14**·HBr in hand, selective debenzoylation was pursued en route to the final API (Scheme 8). As previously

Scheme 8. Completion of the Synthesis



described, incompatibility of the nitrile to hydrogenolysis conditions thwarted our initial efforts. Fortunately, α -chloroethyl chloroformate has been shown to cleave *N*-alkyl bonds under mild conditions while tolerating a variety of sensitive functionalities.³⁶ Following in situ salt break and extraction, application of this method effects debenzoylation to afford amine **19** as its hydrochloride salt. Without isolation, chirality upgrade of the amine with *D*-DBTA furnished salt **2** in >99.75:0.25 er and 67% overall isolated yield for the telescopic process starting from pyridinium salt **13**. Propane phosphonic acid anhydride (T3P)-mediated amide coupling with benzimidazole acid followed by the subsequent hydrochloride salt formation yielded target compound **1** in 76% yield over two steps.

CONCLUSIONS

An efficient enantioselective synthesis of 11 β -HSD-1 inhibitor **1** was developed starting from inexpensive starting materials utilizing low catalyst loadings and excellent step-economy. The total synthesis of the target molecule was achieved in 7 steps with 38% overall yield starting from 3-bromo-4-methylbenzotrile (**4b**). The key feature of the synthesis is a sequence involving intramolecular direct C–H arylation to construct the tricyclic indenopyridine and subsequent asymmetric hydrogenation of the resulting fused indenopyridinium salt. The key asymmetric hydrogenation process was achieved by designing a unique, rigid *P,N*-ligand MeO-BoQPhos. With a low catalyst loading of 1000 ppm [Ir(COD)Cl]₂, the enantio-, diastereo-, and chemoselective reduction of three contiguous double bonds of compound **13**, including a most challenging tetra-substituted alkene intermediate, was accomplished. This concise and innovative synthetic approach avoided functional group manipulation of the labile nitrile moiety and accelerated the production of **1** on multikilogram scale for clinical studies of this diabetes drug candidate.

ASSOCIATED CONTENT

Supporting Information

The Supporting Information is available free of charge on the ACS Publications website at DOI: 10.1021/jacs.6b09764.

Experimental procedures, NMR spectra, chromatograms, calculation data, kinetics data (PDF)

AUTHOR INFORMATION

Corresponding Authors

*E-mail: xudongwei@yahoo.com.

*E-mail: bo.qu@boehringer-ingenelheim.com.

Present Address

W.T.: Shanghai Institute of Organic Chemistry, Chinese Academy of Sciences, 345 Lingling Road, Shanghai 200032, PR China.

Notes

The authors declare no competing financial interest.

ACKNOWLEDGMENTS

We thank the National Institutes of Health (GM087605 to M.C.K.) for financial support. Computational support for the intramolecular cyclization was provided by XSEDE on SDSC Gordon (TG-CHE120052).

REFERENCES

- (1) World Health Organization. *Global status report on non-communicable diseases 2014*; World Health Organization: Geneva, Switzerland, 2014.
- (2) (a) World Health Organization. *Global Health Estimates: Deaths by Cause, Age, Sex and Country, 2000–2012*; World Health Organization: Geneva, Switzerland, 2014. (b) Centers for Disease Control and Prevention. *National Diabetes Statistics Report: Estimates of Diabetes and Its Burden in the United States, 2014*; U.S. Department of Health and Human Services: Atlanta, GA, 2014.
- (3) Eckhardt, M.; Peters, S.; Mar, H.; Himmelsbach, F. Patent WO 2011/057054 A1, 2011.
- (4) (a) Burns, N. Z.; Krylova, I. N.; Hannoush, R. N.; Baran, P. S. *J. Am. Chem. Soc.* **2009**, *131*, 9172–9173. (b) Cook, C. E.; Jump, J. M.; Zhang, P.; Stephens, J. R.; Fail, P. A.; Lee, Y.-W.; Wani, M. C. U.S. Patent US 005952336A, 1999.
- (5) (a) Qu, B.; Saha, A.; Savoie, J.; Wei, X.; Yee, N. K. Patent WO 2013/25664, 2013. (b) Desrosiers, J.-N.; Li, Z.; Qu, B.; Savoie, J.; Senanayake, C. H.; Wei, X.; Zeng, X. U.S. Patent US 2015/141651, 2015.
- (6) Qu, B.; Samankumara, L. P.; Savoie, J.; Fandrick, D. R.; Haddad, N.; Wei, X.; Ma, S.; Lee, H.; Rodriguez, S.; Busacca, C. A.; Yee, N. K.; Song, J. J.; Senanayake, C. H. *J. Org. Chem.* **2014**, *79*, 993–1000.
- (7) (a) Bailey, P. D.; Millwood, P. A.; Smith, P. D. *Chem. Commun.* **1998**, 633–640. (b) Hong, S.; Kawaoka, A. M.; Marks, T. J. *J. Am. Chem. Soc.* **2003**, *125*, 15878–15892. (c) Leighty, M. W.; Georg, G. I. *ACS Med. Chem. Lett.* **2011**, *2*, 313–315. (d) Rueping, M.; Hubener, L. *Synlett* **2011**, *2011*, 1243–1246. (e) Subba Reddy, B. V.; Ghanty, S.; Reddy, N. S. S.; Reddy, Y. J.; Yadav, J. S. *Synth. Commun.* **2014**, *44*, 1658–1663. (f) Hamilton, J. Y.; Sarlah, D.; Carreira, E. M. *Angew. Chem., Int. Ed.* **2015**, *54*, 7644–7647. (g) Tseng, C.-C.; Greig, I. R.; Harrison, W. T. A.; Zanda, M. *Synthesis* **2015**, *48*, 73–78.
- (8) (a) Gaich, T.; Baran, P. S. *J. Org. Chem.* **2010**, *75*, 4657–4673. (b) Wender, P. A. *Nat. Prod. Rep.* **2014**, *31*, 433–440.
- (9) (a) Wang, Q.; Huang, W.; Yuan, H.; Cai, Q.; Chen, L.; Lv, H.; Zhang, X. *J. Am. Chem. Soc.* **2014**, *136*, 16120–16123. (b) Molinaro, C.; Scott, J. P.; Shevlin, M.; Wise, C.; Ménard, A.; Gibb, A.; Junker, E. M.; Lieberman, D. *J. Am. Chem. Soc.* **2015**, *137*, 999–1006.
- (10) Tang, W.; Qu, B.; Capacci, A. G.; Rodriguez, S.; Wei, X.; Haddad, N.; Narayanan, B.; Ma, S.; Grinberg, N.; Yee, N. K.; Krishnamurthy, D.; Senanayake, C. H. *Org. Lett.* **2010**, *12*, 176–179.

- (11) (a) Tang, W.; Capacci, A. G.; Wei, X.; Li, W.; White, A.; Patel, N. D.; Savoie, J.; Gao, J. J.; Rodriguez, S.; Qu, B.; Haddad, N.; Lu, B. Z.; Krishnamurthy, D.; Yee, N. K.; Senanayake, C. H. *Angew. Chem., Int. Ed.* **2010**, *49*, 5879–5883. (b) Fandrick, D. R.; Fandrick, K. R.; Reeves, J. T.; Tan, Z.; Tang, W.; Capacci, A. G.; Rodriguez, S.; Song, J. J.; Lee, H.; Yee, N. K.; Senanayake, C. H. *J. Am. Chem. Soc.* **2010**, *132*, 7600–7601. (c) Tang, W.; Capacci, A. G.; White, A.; Ma, S.; Rodriguez, S.; Qu, B.; Savoie, J.; Patel, N. D.; Wei, X.; Haddad, N.; Grinberg, N.; Yee, N. K.; Krishnamurthy, D.; Senanayake, C. H. *Org. Lett.* **2010**, *12*, 1104–1107. (d) Rodriguez, S.; Qu, B.; Haddad, N.; Reeves, D. C.; Tang, W.; Lee, H.; Krishnamurthy, D.; Senanayake, C. H. *Adv. Synth. Catal.* **2011**, *353*, 533–537. (e) Xu, G.; Fu, W.; Liu, G.; Senanayake, C. H.; Tang, W. *J. Am. Chem. Soc.* **2014**, *136*, 570–573. (f) Qu, B.; Mangunuru, H. P. R.; Wei, X.; Fandrick, K. R.; Desrosiers, J.-N.; Sieber, J. D.; Kurouski, R.; Haddad, N.; Samankumara, L. P.; Lee, H.; Savoie, J.; Ma, S.; Grinberg, N.; Sarvestani, M.; Yee, N. K.; Song, J. J.; Senanayake, C. H. *Org. Lett.* **2016**, *18*, 4920–4923.
- (12) For reviews, see (a) Alberico, D.; Scott, M. E.; Lautens, M. *Chem. Rev.* **2007**, *107*, 174–238. (b) Ackermann, L.; Vicente, R.; Kapdi, A. R. *Angew. Chem., Int. Ed.* **2009**, *48*, 9792–9826.
- (13) For the examples on intramolecular quinoline directed C-3 arylation, see (a) Singh, S. K.; Ruchelmann, A. L.; Li, T.-K.; Liu, A.; Liu, L. F.; LaVoie, E. J. *J. Med. Chem.* **2003**, *46*, 2254–2257. (b) Meyers, C.; Rombouts, G.; Loones, K. T. J.; Coelho, A.; Maes, B. U. W. *Adv. Synth. Catal.* **2008**, *350*, 465–470.
- (14) (a) Furukawa, N.; Tsuruoka, M.; Fujihara, H. *Heterocycles* **1986**, *24*, 3337–3340. (b) Niwa, T.; Yorimitsu, H.; Oshima, K. *Angew. Chem., Int. Ed.* **2007**, *46*, 2643–2645. (c) Shang, R.; Yang, Z.-W.; Wang, Y.; Zhang, S.-L.; Liu, L. *J. Am. Chem. Soc.* **2010**, *132*, 14391–14393. (d) Zhu, F.; Wang, Z.-X. *J. Org. Chem.* **2014**, *79*, 4285–4292. (e) Kianmehr, E.; Faghih, N.; Khan, K. M. *Org. Lett.* **2015**, *17*, 414–417.
- (15) (a) Busacca, C. A.; Wei, X.; Haddad, N.; Kapadia, S.; Lorenz, J. C.; Saha, A. K.; Varsolona, R. J.; Berkenbusch, T.; Campbell, S. C.; Farina, V.; Feng, X.; Gonnella, N. C.; Grinberg, N.; Jones, P.-J.; Lee, H.; Li, Z.; Niemeier, O.; Samstag, W.; Sarvestani, M.; Schroeder, J.; Smoliga, J.; Spinelli, E. M.; Vitous, J.; Senanayake, C. H. *Asian J. Org. Chem.* **2012**, *1*, 80–89. (b) Wei, X.; Shu, C.; Haddad, N.; Zeng, X.; Patel, N. D.; Tan, Z.; Liu, J.; Lee, H.; Shen, S.; Campbell, S.; Varsolona, R. J.; Busacca, C. A.; Hossain, A.; Yee, N. K.; Senanayake, C. H. *Org. Lett.* **2013**, *15*, 1016–1019.
- (16) E-configuration of the free base **8** was confirmed by NMR analyses (See the [Supporting Information](#)). Compound **8** decomposes (polymerization) gradually in air at rt.
- (17) Desrosiers, J.-N.; Wei, X.; Gutierrez, O.; Savoie, J.; Qu, B.; Zeng, X.; Lee, H.; Grinberg, N.; Haddad, N.; Yee, N. K.; Roschangar, F.; Song, J. J.; Kozlowski, M. C.; Senanayake, C. H. *Chem. Sci.* **2016**, *7*, 5581–5586.
- (18) The Ni-catalyzed conditions for substrate **7b** led to lower yields than those of the Pd-catalyzed system.
- (19) Frisch, M. J.; Trucks, G. W.; Schlegel, H. B.; Scuseria, G. E.; Robb, M. A.; Cheeseman, J. R.; Scalmani, G.; Barone, V.; Mennucci, B.; Petersson, G. A.; Nakatsuji, H.; Caricato, M.; Li, X.; Hratchian, H. P.; Izmaylov, A. F.; Bloino, J.; Zheng, G.; Sonnenberg, J. L.; Hada, M.; Ehara, M.; Toyota, K.; Fukuda, R.; Hasegawa, J.; Ishida, M.; Nakajima, T.; Honda, Y.; Kitao, O.; Nakai, H.; Vreven, T.; Montgomery, J. A., Jr.; Peralta, J. E.; Ogliaro, F.; Bearpark, M.; Heyd, J. J.; Brothers, E.; Kudin, K. N.; Staroverov, V. N.; Kobayashi, R.; Normand, J.; Raghavachari, K.; Rendell, A.; Burant, J. C.; Iyengar, S. S.; Tomasi, J.; Cossi, M.; Rega, N.; Millam, J. M.; Klene, M.; Knox, J. E.; Cross, J. B.; Bakken, V.; Adamo, C.; Jaramillo, J.; Gomperts, R.; Stratmann, R. E.; Yazyev, O.; Austin, A. J.; Cammi, R.; Pomelli, C.; Ochterski, J. W.; Martin, R. L.; Morokuma, K.; Zakrzewski, V. G.; Voth, G. A.; Salvador, P.; Dannenberg, J. J.; Dapprich, S.; Daniels, A. D.; Farkas, O.; Foresman, J. B.; Ortiz, J. V.; Cioslowski, J.; Fox, D. J. *Gaussian 09*, revision C.01; Gaussian, Inc.: Wallingford, CT, 2009.
- (20) (a) Hay, P. J.; Wadt, W. R. *J. Chem. Phys.* **1985**, *82*, 270–283. (b) Hay, P. J.; Wadt, W. R. *J. Chem. Phys.* **1985**, *82*, 299–310.
- (21) About 5% of the *trans*-isomer was generated during heterogeneous reduction. It was isolated from mother liquor and characterized (see the [Supporting Information](#)).
- (22) (a) Wang, D.-S.; Chen, Q.-A.; Li, W.; Yu, C.-B.; Zhou, Y.-G.; Zhang, X. *J. Am. Chem. Soc.* **2010**, *132*, 8909–8911. (b) Dobreiner, G. E.; Nova, A.; Schley, N. D.; Hazari, N.; Miller, S. J.; Eisenstein, O.; Crabtree, R. H. *J. Am. Chem. Soc.* **2011**, *133*, 7547–7562. (c) Woodmansee, D. H.; Pfaltz, A. *Top. Organomet. Chem.* **2011**, *34*, 31–76. (d) Wang, D.-S.; Chen, Q.-A.; Lu, S.-M.; Zhou, Y.-G. *Chem. Rev.* **2012**, *112*, 2557–2590. (e) Liu, Y.; Du, H. *J. Am. Chem. Soc.* **2013**, *135*, 12968–12971. (f) Zhao, D.; Glorius, F. *Angew. Chem., Int. Ed.* **2013**, *52*, 9616–9618. (g) Huang, W.-X.; Liu, L.-J.; Wu, B.; Feng, G.-S.; Wang, B.; Zhou, Y.-G. *Org. Lett.* **2016**, *18*, 3082–3085. (h) Gualandi, A.; Savoia, D. *RSC Adv.* **2016**, *6*, 18419–18451.
- (23) (a) Glorius, F.; Spielkamp, N.; Holle, S.; Goddard, R.; Lehmann, C. W. *Angew. Chem., Int. Ed.* **2004**, *43*, 2850–2852. (b) Legault, C. Y.; Charette, A. B. *J. Am. Chem. Soc.* **2005**, *127*, 8966–8967. (c) Ye, Z.-S.; Chen, M.-W.; Chen, Q.-A.; Shi, L.; Duan, Y.; Zhou, Y.-G. *Angew. Chem., Int. Ed.* **2012**, *51*, 10181–10184. (d) Chang, M.; Huang, Y.; Liu, S.; Chen, Y.; Kraska, S. W.; Davies, I. W.; Zhang, X. *Angew. Chem., Int. Ed.* **2014**, *53*, 12761–12764. (e) Kita, Y.; Iimuro, A.; Hida, S.; Mashima, K. *Chem. Lett.* **2014**, *43*, 284–286. (f) Chen, M.-W.; Ye, Z.-S.; Chen, Z.-P.; Wu, B.; Zhou, Y.-G. *Org. Chem. Front.* **2015**, *2*, 586–589. (g) Zhou, Q.; Zhang, L.; Meng, W.; Feng, X.; Yang, J.; Du, H. *Org. Lett.* **2016**, *18*, 5189–5191.
- (24) Li, Z.-W.; Wang, T.-L.; He, Y.-M.; Wang, Z.-J.; Fan, Q.-H.; Pan, J.; Xu, L.-J. *Org. Lett.* **2008**, *10*, 5265–5268.
- (25) (a) Wang, Q.; Huang, W.; Yuan, H.; Cai, Q.; Chen, L.; Lv, H.; Zhang, X. *J. Am. Chem. Soc.* **2014**, *136*, 16120–16123. (b) Molinaro, C.; Scott, J. P.; Shevlin, M.; Wise, C.; Ménard, A.; Gibb, A.; Junker, E. M.; Lieberman, D. *J. Am. Chem. Soc.* **2015**, *137*, 999–1006.
- (26) Lei, A.; Chen, M.; He, M.; Zhang, X. *Eur. J. Org. Chem.* **2006**, *2006*, 4343–4347.
- (27) Crabtree, R. H. *Acc. Chem. Res.* **1979**, *12*, 331–337.
- (28) Qu, B.; Samankumara, L. P.; Ma, S.; Fandrick, K. R.; Desrosiers, J.-N.; Rodriguez, S.; Li, Z.; Haddad, N.; Han, Z. S.; McKellop, K.; Pennino, S.; Grinberg, N.; Gonnella, N. C.; Song, J. J.; Senanayake, C. H. *Angew. Chem., Int. Ed.* **2014**, *53*, 14428–14432.
- (29) Busacca, C. A.; Qu, B.; Grät, N.; Fandrick, K. R.; Saha, A. K.; Marsini, M.; Reeves, D.; Haddad, N.; Eriksson, M.; Wu, J.-P.; Grinberg, N.; Lee, H.; Li, Z.; Lu, B.; Chen, D.; Hong, Y.; Ma, S.; Senanayake, C. H. *Adv. Synth. Catal.* **2013**, *355*, 1455–1463.
- (30) Free base indenopyridine **9** has demonstrated similar reactivity at high catalyst load and the same enantioselectivity at 85:15 er, but with formation of about 10% dimeric impurity resulted from nonchemoselective nitrile reduction.
- (31) Dobreiner, G. E.; Nova, A.; Schley, N. D.; Hazari, N.; Miller, S. J.; Eisenstein, O.; Crabtree, R. H. *J. Am. Chem. Soc.* **2011**, *133*, 7547–7562.
- (32) (a) Becke, A. D. *J. Chem. Phys.* **1993**, *98*, 5648–5652. (b) Lee, C.; Yang, W.; Parr, R. G. *Phys. Rev. B: Condens. Matter Mater. Phys.* **1988**, *37*, 785–789.
- (33) Dunning, T. H., Jr.; Hay, P. J. In *Modern Theoretical Chemistry*; Schaefer, H. F., III, Ed.; Methods of Electronic Structure Theory series, Vol. 3; Plenum: New York, 1977; pp 1–28.
- (34) (a) Martín, M.; Sola, E.; Tejero, S.; Andrés, J. L.; Oro, L. A. *Chem. - Eur. J.* **2006**, *12*, 4043–4056. (b) Martín, M.; Sola, E.; Tejero, S.; López, J. A.; Oro, L. A. *Chem. - Eur. J.* **2006**, *12*, 4057–4068.
- (35) Hopmann, K. H.; Bayer, A. *Organometallics* **2011**, *30*, 2483–2497.
- (36) (a) Olofson, R. A.; Martz, J. T.; Senet, J.-P.; Piteau, M.; Malfroot, T. *J. Org. Chem.* **1984**, *49*, 2081–2082. (b) Yang, B. V.; O'Rourke, D.; Li, J. *Synlett* **1993**, *1993*, 195–196.